Pergamon

Int. J. Solids Structures Vol. 34, No. 14, pp. 1797–1822, 1997

0020-7683/97 $17.00 + .00

PII: S0020-7683(96)00114-X

ANALYTIC AND FINITE ELEMENT SOLUTIONS FOR BENDING AND BUCKLING OF ORTHOTROPIC RECTANGULAR PLATES

G. BAO and W. JIANG
Department of Mechanical Engineering, The Johns Hopkins University, Baltimore, MD 21218, U.S.A.

and

J. C. ROBERTS
Applied Physics Laboratory, The Johns Hopkins University, Laurel, MD 20723, U.S.A.

(*Received* 17 *April* 1995; *in revised form* 28 *May* 1996)

Abstract— This paper presents a critical review of analytic solutions for bending and buckling of flat, rectangular, orthotropic thin plates. Considered are plates with all edges simply supported, two edges simply supported and two edges clamped, and all edges clamped. An orthotropy rescaling technique is employed to simplify the analysis. The material orthotropy is characterized by two non-dimensional parameters, $\lambda = D_{22}/D_{11}$ and $\eta = (D_{12} + 2D_{66})/\sqrt{D_{11}D_{22}}$. When $\eta \approx 1$, many solutions for orthotropic plates can be obtained directly from the corresponding isotropic results. Systematic comparisons with finite element solutions are made for the critical buckling load of a plate under in-plane compression, and for deflection and stresses in a plate under out-of-plane uniform pressure. It is found that for plates with all edges clamped, the analytic solution for critical buckling load is neither accurate nor conservative; a better solution needs to be developed for design purposes. The validity of the thin plate theory solutions over a range of plate thicknesses is also examined. © 1997 Elsevier Science Ltd.

1. INTRODUCTION

With progress in composite materials technology, composite plates made of solid laminates, sandwich laminates, and laminates reinforced with stiffeners are widely used in aerospace and marine structures. The analysis of bending and buckling of composite plates is critical to the safe-design of these structures. Unlike plates made of conventional materials such as steel, composite plates such as those made of fiber reinforced plastics are inherently anisotropic and inhomogeneous, their bending and buckling deformations are more complicated. Analytic solutions to the bending and buckling problems of composite plates are desirable since they provide convenient tools for the design of composite structures. However, these solutions are based on certain assumptions and often approximate in nature; a close examination of their accuracy is thus needed.

The bending and buckling of rectangular plates has been a subject of study in solid mechanics for more than a century. Many exact solutions for isotropic linear elastic thin plates have been developed; most of them can be found in Timoshenko's monographs (Timoshenko and Woinowsky-Krieger, 1959; Timoshenko and Gere, 1961). Exact and approximate solutions for anisotropic plates and laminated plates have also been derived and subsequently compiled by Lekhnitskii (1968) and by Whitney (1987). However, even for a thin, homogeneous orthotropic plate, the analytic solutions given in the open literature are incomplete. Further, owing to material orthotropy, the form of the solution to the bending problem depends on the plate rigidities; its determination involves solving a fourth order algebraic equation. To simplify the analysis, a better handling of material orthotropy is called for.

To benefit the designers of composite plate structures, in this article, analytic solutions for bending and buckling of homogeneous orthotropic thin plates are reviewed. The plate is taken to be flat, rectangular, with edges aligned along material principal directions. An

ropy rescaling technique is introduced so that only one nondimensional material eter appears in the governing equation; the eigenvalues involved in the buckling and ...g problems are solved in a closed-form. Existing analytic solutions, with mistakes ...cted, are compiled using two nondimensional material parameters; analytic solutions ...annot be found in the open literature are derived.

The accuracy of the analytic solutions compiled and developed in this study varies: those for simply supported plates are exact, others approximate. Further, owing to the thin-plate theory assumptions, all the analytic solutions are approximate when the plate thickness becomes large. To cross-check the accuracy of the analytic approximate solutions, and to identify the range of plate thicknesses over which the analytic solutions are valid, systematic finite element calculations were performed for plates with different aspect ratios and thicknesses to obtain the critical buckling loads under in-plane uniaxial compression, and deflections and stresses under out-of-plane uniform pressure. All the finite element results were obtained using the commercial finite element code ABAQUS. Specifically, 800 shell elements of type S4R, which is valid for both thin and thick plates, were used for each calculation; the mesh sensitivity and convergence check has been reported in Jiang *et al.* (1996).

2. ORTHOTROPY RESCALING

Assume that the thin plate with length a, width b and thickness h is homogeneous, orthotropic, with material principal direction 1 and 2, as depicted in Fig. 1. Under plane stress conditions relative to the 1 and 2 axes, the stress–strain behavior of the material can be given by

$$\begin{aligned} \varepsilon_{11} &= b_{11}\sigma_{11} + b_{12}\sigma_{22} \\ \varepsilon_{22} &= b_{12}\sigma_{11} + b_{22}\sigma_{22} \\ \varepsilon_{12} &= b_{66}\sigma_{12} \end{aligned} \tag{1}$$

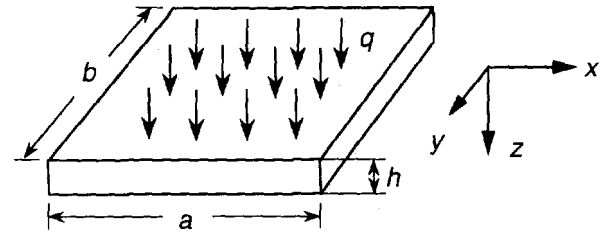

(a)

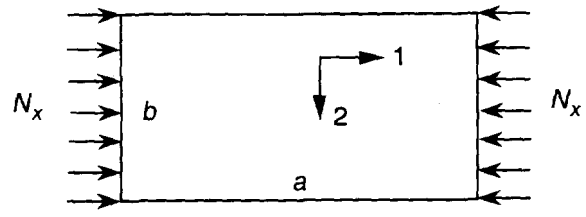

(b)

Fig. 1. Schematic of a flat, orthotropic, rectangular plate (a) under out-of-plane uniform pressure and (b) under in-plane uniaxial compression. Shown also are the dimensions of the plate and the Cartesian coordinates.

where b_{ij}'s are components of the compliance matrix. In terms of engineering constants, we have

$$b_{11} = \frac{1}{E_1}, \quad b_{22} = \frac{1}{E_2}, \quad b_{12} = \frac{-\nu_{12}}{E_1}, \quad b_{66} = \frac{1}{G_{12}} \tag{2}$$

where E_1 and E_2 are Young's moduli in 1- and 2-directions, respectively, ν_{12} is Poisson's ratio and G_{12} is the shear modulus. The general treatment of 3-dimensional material anisotropy can be found in Lekhnitskii (1981). A standard, x, y, z coordinate system is introduced such that the x- and y-axes coincide with the 1- and 2-axes, respectively, as shown in Fig. 1.

Based on the usual assumptions in the theory of the bending of thin plates, the governing equation for displacement w of the plate in the z-direction is

$$D_{11}\frac{\partial^4 w}{\partial x^4} + 2(D_{12} + 2D_{66})\frac{\partial^4 w}{\partial x^2 \partial y^2} + D_{22}\frac{\partial^4 w}{\partial y^4} = F(x, y) \tag{3}$$

where D_{ij}'s are the flexural rigidities of the plate given by

$$D_{11} = \frac{E_1 h^3}{12(1-\nu_{12}\nu_{21})}, \quad D_{22} = \frac{E_2 h^3}{12(1-\nu_{12}\nu_{21})},$$
$$D_{12} = \frac{\nu_{21} E_1 h^3}{12(1-\nu_{12}\nu_{21})}, \quad D_{66} = \frac{G_{12} h^3}{12} \tag{4}$$

with $\nu_{21} = \nu_{12}E_2/E_1$. For inhomogeneous materials such as laminates, the D_{ij}'s can be obtained from the properties of the plies following a standard procedure (Jones, 1975). The function $F(x, y)$ on the right hand side of (3) depends on the problem under consideration. For example, for a plate under uniform out-of-plane pressure q as illustrated in Fig. 1a, we have

$$F(x, y) = q. \tag{5}$$

For a plate under in-plane compression N_x in the x-direction as shown in Fig. 1b, $F(x, y)$ is given by

$$F(x, y) = -N_x \frac{\partial^2 w}{\partial x^2}. \tag{6}$$

Under free-vibration of the plate,

$$F(x, y) = -\rho \frac{\partial^2 w}{\partial t^2} \tag{7}$$

where ρ is the density of the plate integrated over its thickness.

Equation (3) can be rewritten as

$$\frac{\partial^4 w}{\partial x^4} + 2\eta\lambda^2 \frac{\partial^4 w}{\partial x^2 \partial y^2} + \lambda^4 \frac{\partial^4 w}{\partial y^4} = \frac{F(x, y)}{D_{11}} \tag{8}$$

where

$$\lambda = \frac{D_{22}}{D_{11}}, \quad \eta = \frac{D_{12} + 2D_{66}}{\sqrt{D_{11} D_{22}}} \tag{9a}$$

are non-dimensional parameters characterizing material orthotropy. For a homogeneous, orthotropic plate, (9a) can be rewritten as

$$\lambda = \frac{E_2}{E_1}, \quad \eta = \frac{2G_{12}(1 - \nu_{12}\nu_{21})}{\sqrt{E_1 E_2}} + \sqrt{\nu_{12}\nu_{21}}. \tag{9b}$$

It can be shown readily from the positive-definiteness of the strain energy that

$$0 < \lambda < \infty, \quad -1 < \eta < \infty. \tag{9c}$$

However, for most engineering materials such as fiber reinforced plastics, $0 < \eta < 5$ (Lekhnitskii, 1981).

Introducing an orthotropy rescaling of the y-coordinate

$$\psi = \lambda^{1/4} y, \tag{10}$$

eqn (8) becomes

$$\frac{\partial^4 w}{\partial x^4} + 2\eta \frac{\partial^4 w}{\partial x^2 \partial \psi^2} + \frac{\partial^4 w}{\partial \psi^4} = \frac{F(x, \lambda^{1/4}\psi)}{D_{11}}. \tag{11}$$

The forms of eqns (8) and (11) indicate that although the deflection of a thin orthotropic plate depends on four elastic constants E_1, E_2, ν_{12} and G_{12}, only two non-dimensional parameters λ and η are involved in the analysis. Note that, for bending, buckling and free vibration problems defined by (5), (6), (7) and (11), only η appears in the governing equation. In particular, if an orthotropic plate has $\eta \approx 1$, the form of eqn (11) becomes identical to that for an isotropic plate. Therefore, *all existing solutions for an isotropic plate* can be converted readily to *solutions for an orthotropic plate* with $\eta \approx 1$.

The orthotropy rescaling in eqns (9)–(11) has important implications. If a plate has width b, then, after rescaling in the y-direction, the width of the plate becomes $\hat{b} = \lambda^{-1/4} b$, and the adjusted aspect ratio R of the plate in the new x–ψ system is related to the original plate aspect ratio $r = a/b$ by

$$R = a/\hat{b} = \lambda^{1/4} a/b = \lambda^{1/4} r. \tag{12}$$

Equation (12) implies that the effect of E_2/E_1 is mainly to change the aspect ratio of the plate. Consequently, for any orthotropic plate with stress–strain behavior (1), it is sufficient to solve (11) together with the adjusted plate aspect ratio R. The analysis is thus simplified. Orthotropy rescaling similar to that defined in (9) and (10) has been applied to fracture mechanics problems by Suo *et al.* (1991) and Bao *et al.* (1992), to buckling of orthotropic plate by Brunelle and Oyibo (1983) and to free-vibration of orthotropic plates by Yu and Cleghorn (1993). Parameters similar to λ and η have also been used by March and Smith (1945) in a buckling analysis, by Huber (1929) for bending of a plate with $\eta = 1$, and by Smith (1990) in his studies of bending and stretching of orthotropic plates.

In the sections that follow, we will consider solutions to the governing equation

$$\frac{\partial^4 w}{\partial x^4} + 2\eta \frac{\partial^4 w}{\partial x^2 \partial y^2} + \frac{\partial^4 w}{\partial y^4} = \frac{F(x, \lambda^{1/4} y)}{D_{11}} \tag{13}$$

with $F(x, \lambda^{1/4} y)$ specified in (5) and (6) for bending and buckling of the plate. For convenience, in the following, y is used instead of ψ. Free-vibration of an orthotropic plate

can be analyzed in a similar fashion but will not be considered here. The boundary conditions associated with (13) are:

(i) Plates with all edges simply supported

$$w|_{x=0,a} = 0, \quad w|_{y=0,b} = 0$$
$$\left.\frac{\partial^2 w}{\partial x^2}\right|_{x=0,a} = 0, \quad \left.\frac{\partial^2 w}{\partial y^2}\right|_{y=0,b} = 0. \tag{14a}$$

(ii) Plates with two edges ($x = 0, a$) clamped and others simply supported

$$w|_{x=0,a} = 0, \quad w|_{y=0,b} = 0$$
$$\left.\frac{\partial w}{\partial x}\right|_{x=0,a} = 0, \quad \left.\frac{\partial^2 w}{\partial y^2}\right|_{y=0,b} = 0. \tag{14b}$$

(iii) Plates with all edges clamped

$$w|_{x=0,a} = 0, \quad w|_{y=0,b} = 0$$
$$\left.\frac{\partial w}{\partial x}\right|_{x=0,a} = 0, \quad \left.\frac{\partial w}{\partial y}\right|_{y=0,b} = 0. \tag{14c}$$

Once the deflection $w(x, y)$ is solved from (13) together with boundary conditions (14), the moment resultants M_x and M_y can be obtained using

$$M_x = -D_{11}\frac{\partial^2 w}{\partial x^2} - \frac{D_{12}}{\sqrt{\lambda}}\frac{\partial^2 w}{\partial y^2} \tag{15a}$$

$$M_y = -D_{12}\frac{\partial^2 w}{\partial x^2} - \frac{D_{22}}{\sqrt{\lambda}}\frac{\partial^2 w}{\partial y^2} \tag{15b}$$

where the effect of orthotropy rescaling in the y-direction is included. The normal stresses at the surfaces of the plate are related to M_x and M_y by

$$\sigma_x = \frac{6M_x}{h^2}, \quad \sigma_y = \frac{6M_y}{h^2}. \tag{16}$$

3. BUCKLING UNDER UNIAXIAL COMPRESSION

Consider a rectangular orthotropic plate under in-plane compression N_x applied on the edges $x = 0, a$, as shown in Fig. 1b. The critical buckling stress σ_{cr} depends on the geometry and material of the plate, and the buckling mode. In a nondimensional form, σ_{cr} can be expressed as

$$\sigma_{cr}/\sigma_0 = \phi(R, \eta, m) \tag{17}$$

where σ_0 is a reference buckling stress

$$\sigma_0 = \frac{\pi^2\sqrt{D_{11}D_{22}}}{b^2 h}, \tag{18}$$

$R = \lambda^{1/4}a/b$ is the adjusted plate aspect ratio, and m is the number of half-waves in the

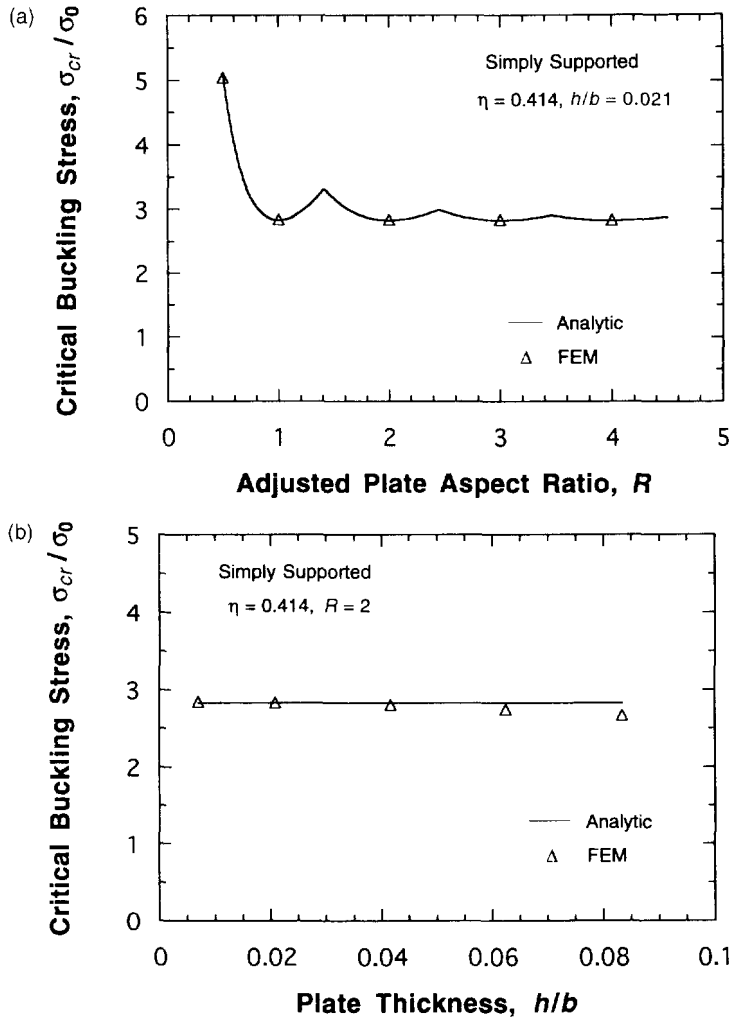

Fig. 2. Normalized critical buckling stress σ_{cr}/σ_0 as a function of (a) the adjusted plate aspect ratio $R = (D_{22}/D_{11})^{1/4} a/b$ and (b) the nondimensional plate thickness h/b for plates with all edges simply supported. The analytic solution is shown as the solid line and the finite element solution as points.

loading direction (x-direction). Note that the dependence of σ_{cr}/σ_0 on λ is given entirely through R.

3.1. *Plates with all edges simply supported*

For a plate with all edges simply supported, the exact solution for critical buckling stress σ_{cr} is given by (e.g., Whitney, 1987)

$$\frac{\sigma_{cr}}{\sigma_0} = \frac{R^2}{m^2} + \frac{m^2}{R^2} + 2\eta. \tag{19}$$

It is readily determined from (19) that a plate will buckle in m half-waves if

$$\sqrt{m(m-1)} \leqslant R \leqslant \sqrt{m(m+1)}, \quad m \geqslant 1; \tag{20}$$

i.e., the transition from m to $m+1$ half-waves occurs when $R = \sqrt{m(m+1)}$. Displayed in Fig. 2a is the comparison between analytic and finite element solutions for σ_{cr}/σ_0 for plates with $h/b = 0.021$ with different adjusted aspect ratios R. The agreement is seen to be excellent. Since the analytic solution (19) is exact for thin plates, the high accuracy of the finite element model is established.

As a direct consequence of the thin plate theory assumptions, the normalized critical buckling stress σ_{cr}/σ_0 given in (19) does not depend on plate thickness h. However, in general, as the plate thickness increases, the error owing to the assumptions in thin plate theory can be large. To uncover the range of plate thicknesses within which (19) is valid, in Fig. 2b, σ_{cr}/σ_0 is plotted against the normalized plate thickness h/b for $R = 2$. The solid line is the prediction made based on (19); the points are computed using the finite element S4R which is valid for both thin and thick plates. It is clear from Fig. 2b that for plates with all edges simply supported, the solution given in (19) is quite accurate for $h/b \leqslant 1/12$.

3.2. *Plates with two loaded edges clamped/others simply supported*

For plates with two loaded edges clamped and two other edges simply supported, the exact solution for critical buckling stress σ_{cr} is derived (Appendix A)

$$\frac{\sigma_{cr}}{\sigma_0} = 2(k+\eta) \tag{21a}$$

where k can be solved from the equation

$$(1+k)\cos[(\lambda_1-\lambda_2)\pi R]+(1-k)\cos[(\lambda_1+\lambda_2)\pi R] = 2 \tag{21b}$$

with

$$\lambda_1 = \sqrt{k+\sqrt{k^2-1}}, \quad \lambda_2 = \sqrt{k-\sqrt{k^2-1}}, \quad k > 1. \tag{21c}$$

Note that there is no η dependence in eqns (21b) and (21c); the solution for k therefore is the same as that for an isotropic plate with aspect ratio R. Following Timoshenko and Gere (1961), the plate will buckle in m half-waves if

$$\sqrt{(m+1)(m-1)} \leqslant R \leqslant \sqrt{m(m+2)}, \quad m \geqslant 1. \tag{22}$$

Using an energy method (Timoshenko and Gere, 1961), an approximate solution for σ_{cr} has been developed (March and Smith, 1945) which gives

$$\text{one half-wave:} \quad \frac{\sigma_{cr}}{\sigma_0} = \frac{3R^2}{4} + \frac{4}{R^2} + 2\eta, \tag{23a}$$

$$m \text{ half-waves:} \quad \frac{\sigma_{cr}}{\sigma_0} = \frac{R^2}{m^2+1} + \frac{m^4+6m^2+1}{(m^2+1)R^2} + 2\eta, \quad m > 1. \tag{23b}$$

Based on eqn (23), a plate with two loaded edges clamped and two other edges simply supported will buckle in one half-wave if

$$R \leqslant (84/11)^{1/4}; \tag{24a}$$

it will buckle in two half-waves if

$$(84/11)^{1/4} \leqslant R \leqslant (54)^{1/4}; \tag{24b}$$

it will buckle in m half-waves ($m > 2$) if

$$(m^4-2m^3+3m^2-2m+6)^{1/4} \leqslant R \leqslant (m^4+2m^3+3m^2+2m+6)^{1/4}. \tag{24c}$$

The transition aspect ratios given by (24) differ slightly from the exact solution (22). For

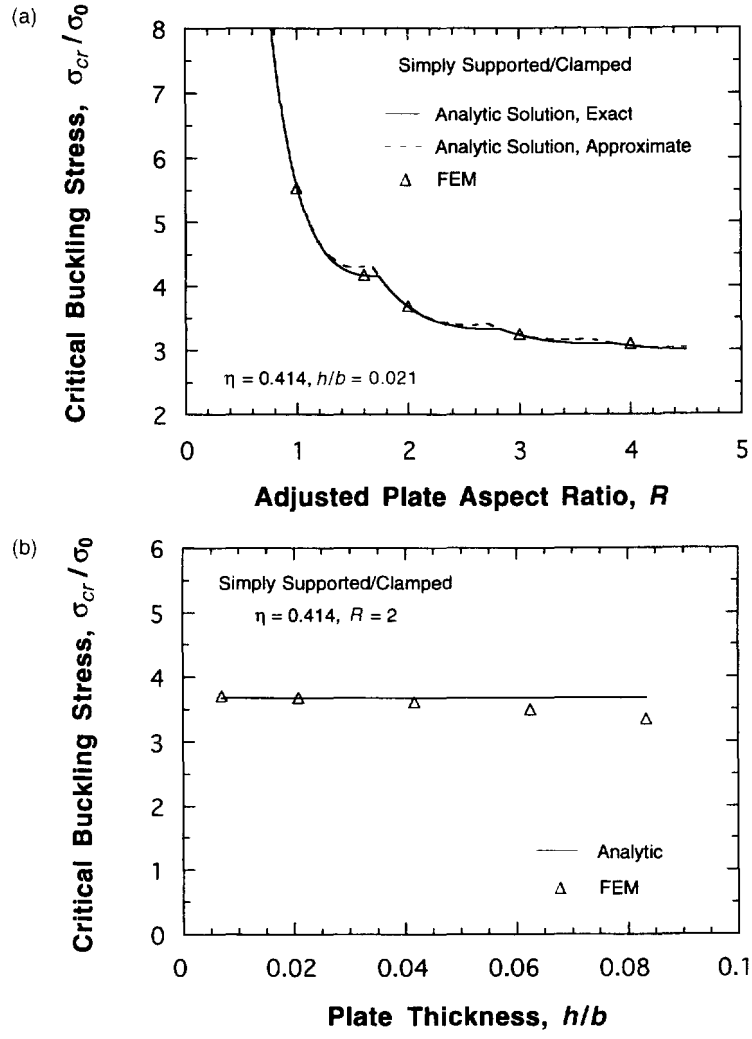

Fig. 3. Normalized critical buckling stress σ_{cr}/σ_0 as a function of (a) the adjusted plate aspect ratio $R = (D_{22}/D_{11})^{1/4} a/b$ and (b) the nondimensional plate thickness h/b for plates with two loaded edges clamped and other edges simply supported. The analytic solution is shown as the solid line and the finite element solution as points. Shown also in (a) as the dashed line is an approximate solution based on an energy method.

example, according to (22), the plate buckles in one half-wave up to $R = 1.732$, while eqn (24a) gives $R = 1.662$.

Shown in Fig. 3a is the normalized critical buckling stress σ_{cr}/σ_0 as a function of the adjusted plate aspect ratio R for $h/b = 0.021$. The solid line is the exact solution obtained from (21), the dashed line is the approximate solution (23), and the points are finite element solutions. The finite element solution is almost identical to the exact analytic solution (21); the approximate analytic solution given in (23) is also quite accurate. It is worth noticing from (21) and (23) that for any value of η other than $\eta = 0.414$ used in the calculation, the two curves shown in Fig. 3a will just move up or down without changing its shape. It is again true that the analytical solution for critical buckling stress σ_{cr} given by (21) or (23) is accurate only for thin plates, as demonstrated in Fig. 3b. For example, when $h = b/12$, the analytic solution (shown as the solid line) for σ_{cr}/σ_0 is about 10% higher than the corresponding finite element solution (shown as points).

3.3. *Plates with all edges clamped*

There exists no exact solution for σ_{cr} for plates with all edges clamped. An estimate for σ_{cr} can be obtained using the following formulae (March and Smith, 1945)

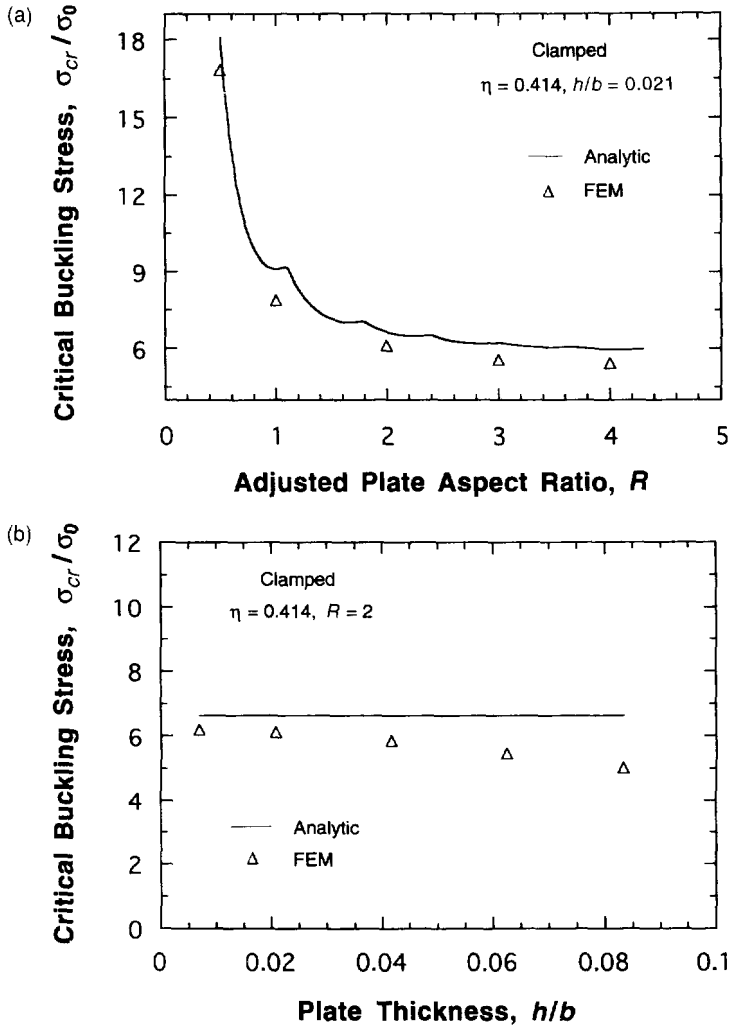

Fig. 4. Normalized critical buckling stress σ_{cr}/σ_0 as a function of (a) the adjusted plate aspect ratio $R = (D_{22}/D_{11})^{1/4} a/b$ and (b) the nondimensional plate thickness h/b for plates with all edges clamped. The analytic solution is shown as the solid line and the finite element solution as points.

$$\text{one half-wave:} \quad \frac{\sigma_{cr}}{\sigma_0} = 4R^2 + \frac{4}{R^2} + \frac{8}{3}\eta, \tag{25a}$$

$$m \text{ half-waves:} \quad \frac{\sigma_{cr}}{\sigma_0} = \frac{16R^2}{3(m^2+1)} + \frac{m^4+6m^2+1}{(m^2+1)R^2} + \frac{8}{3}\eta, \quad m > 1. \tag{25b}$$

It is readily seen from eqn (25) that a plate with all edges clamped will buckle in one half-wave if

$$R \leqslant (63/44)^{1/4}; \tag{26a}$$

it will buckle in two half-waves if

$$(63/44)^{1/4} \leqslant R \leqslant (81/8)^{1/4}; \tag{26b}$$

it will buckle in m half-waves ($m > 2$) if

$$\tfrac{1}{2}[3(m^4 - 2m^3 + 3m^2 - 2m + 6)]^{1/4} \leqslant R \leqslant \tfrac{1}{2}[3(m^4 + 2m^3 + 3m^2 + 2m + 6)]^{1/4}. \tag{26c}$$

To examine the accuracy of the approximate solution (25), the normalized critical buckling stress σ_{cr}/σ_0 is plotted in Fig. 4a as a function of the adjusted plate aspect ratio R

for $h/b = 0.021$ and in Fig. 4b as a function of the plate thickness ratio h/b for $R = 2$. The finite element results are also shown for comparison. Although not exact in the strict mathematical sense, the finite element solutions for σ_{cr} is believed to be very accurate, as demonstrated by Figs 2a and 3a. Evidently, for plates with all edges clamped, the analytic solution given by (25) is not very accurate. Further, the range of the plate thickness ratios within which thin plate theory works well is found to be much narrower. This is due to the high deformation constraint introduced by the clamped edges. Clearly, a better analytic solution for σ_{cr} for plates with all edges clamped needs to be developed. The problem is very challenging due to the mathematical difficulties involved.

In summary, for a plate with all edges simply supported, the exact solution for the critical buckling load is very accurate for plate thickness h up to about $b/12$. For a plate with two loaded edges clamped and other edges simply supported, the exact solution is quite accurate for h up to about $b/16$. However, for a plate with all edges clamped, the approximate closed-form solution for σ_{cr} is found to be inaccurate and non-conservative, even when the plate thickness is not large.

The effects of material orthotropy on the critical buckling load are as follows. Increase the flexural rigidity $\sqrt{D_{11}D_{22}}$ will result in a higher σ_{cr}. The effect of $\lambda = D_{22}/D_{11}$ is just to *modify the plate aspect ratio* in terms of $R = \lambda^{1/4}a/b$; decreasing λ will reduce the number of half-waves and in general increase σ_{cr}. The effect of η is to *move the* σ_{cr} vs R *curve up or down*: the higher the value of η the larger the σ_{cr}.

4. BENDING UNDER UNIFORM PRESSURE

When an orthotropic plate is subjected to out-of-plane uniform pressure q as depicted in Fig. 1a, the maximum deflection Δ occurs in the middle of the plate. In a nondimensional form, Δ can be expressed as

$$\Delta/\Delta_0 = \psi(R, \eta) \tag{27a}$$

where Δ_0 is a reference deflection

$$\Delta_0 = \frac{qb^4}{D_{22}}. \tag{27b}$$

$R = \lambda^{1/4}a/b$ is the adjusted plate aspect ratio. Note that Δ/Δ_0 only depends on R and η, the dependence on λ is entirely through R.

The maximum stresses in an orthotropic plate may or may not occur at the center of the plate, depending on the boundary conditions and material orthotropy. For convenience, in most of the following discussions, only the stresses σ_x and σ_y at the center of the plate are considered. In nondimensional forms, the stresses σ_x and σ_y at the center of the plate can be expressed as

$$\frac{\sigma_x h^2}{qb^2} = \chi_x(R, \lambda, \eta, \nu_{12}), \tag{28a}$$

$$\frac{\sigma_y h^2}{qb^2} = \chi_y(R, \lambda, \eta, \nu_{12}). \tag{28b}$$

The parameters λ and ν_{12} come into play as indicated by eqn (15). The stresses may also depend on ν_{21} but $\nu_{21} = \lambda\nu_{12}$.

4.1. *Plates with all edges simply supported*

4.1.1. *Maximum deflection.* The exact solution for the maximum deflection Δ of the plate under uniform pressure q is given by (Whitney, 1987)

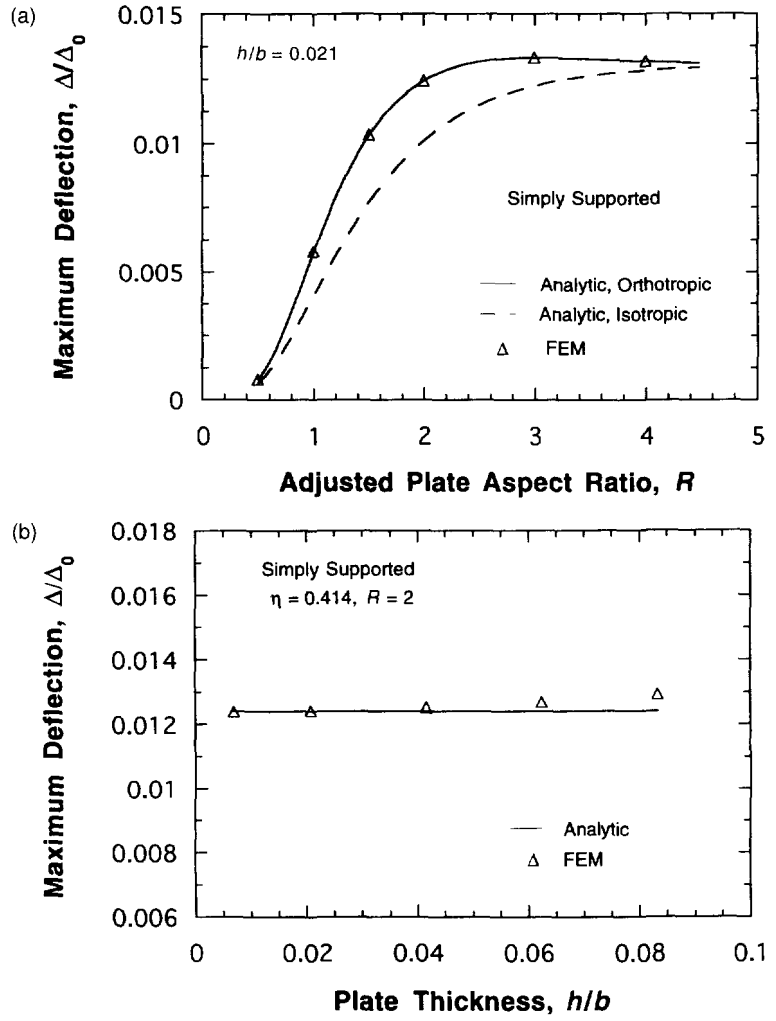

Fig. 5. Normalized maximum deflection Δ/Δ_0 as a function of (a) the adjusted plate aspect ratio $R=(D_{22}/D_{11})^{1/4}a/b$ and (b) the nondimensional plate thickness h/b for plates with all edges simply supported. The analytic solution is shown as the solid line and the finite element solution as points. Shown also in (a) as the dashed line is the corresponding isotropic solution.

$$\frac{\Delta}{\Delta_0}=\frac{16R^4}{\pi^6}\sum_{m=1,3,\ldots}^{\infty}\sum_{n=1,3,\ldots}^{\infty}\frac{(-1)^{(m+n-2)/2}}{D_{mn}} \tag{29}$$

where

$$D_{mn}=m^4+2\eta(mnR)^2+(nR)^4. \tag{30}$$

Plotted in Fig. 5a is the normalized deflection Δ/Δ_0 against the adjusted aspect ratio R of the plate with $h/b=0.021$. The solid line is the analytic solution given by (29) with $\eta=0.414$; the points are finite element results. The isotropic solution ($\lambda=1, \eta=1$) is also shown as the dashed line for comparison. The finite element solution is seen to be very accurate. It is interesting to note that even if $\lambda=1$, i.e., $E_1=E_2$, the effect of material orthotropy ($\eta=0.414$) can be large. When the adjusted plate aspect ratio R is large, say, $R\geqslant 4$, it can be shown (Lekhnitskii, 1968) that the normalized deflection Δ/Δ_0 approaches 5/384.

The governing eqn (3) is based on the thin plate theory assumptions; the solution given in (29), therefore, may be inaccurate for plates with large thicknesses. To show the range of plate thicknesses within which (29) is valid, in Fig. 5b, Δ/Δ_0 is plotted as a function of h/b for $R=2$. The analytic solution for Δ/Δ_0 using eqn (29) is shown as the solid line; it is independent of h. The finite element solutions are shown as points; they are more

accurate. Evidently, even for a plate with $h = b/12$, the relative error ($\sim 4\%$) in the analytic solution for Δ is insignificant.

4.1.2. *Maximum stresses.* When a plate is simply supported at all edges, the maximum stresses σ_x and σ_y occur at the center of the plate. For plates with $-1 < \eta < 1$, it can be shown that under uniform out-of-plane pressure q, σ_x and σ_y are given by

$$\frac{\sigma_x h^2}{qb^2} = \frac{3\nu_{12}}{4} + \frac{24}{\pi^3 \lambda \lambda_1 \lambda_2} \sum_{m=1,3,\ldots}^{\infty} \frac{(-1)^{(m-1)/2}}{m^3 \phi_m} \times \left[(\sqrt{\lambda} - \nu_{21}\eta) \sinh \frac{m\pi\lambda_1 R}{2} \sin \frac{m\pi\lambda_2 R}{2} - 2\nu_{21}\lambda_1\lambda_2 \cosh \frac{m\pi\lambda_1 R}{2} \cos \frac{m\pi\lambda_2 R}{2} \right] \tag{31a}$$

$$\frac{\sigma_y h^2}{qb^2} = \frac{3}{4} + \frac{24}{\pi^3 \lambda_1 \lambda_2} \sum_{m=1,3,\ldots}^{\infty} \frac{(-1)^{(m-1)/2}}{m^3 \phi_m} \times \left[(\nu_{12}\sqrt{\lambda} - \eta) \sinh \frac{m\pi\lambda_1 R}{2} \sin \frac{m\pi\lambda_2 R}{2} - 2\lambda_1\lambda_2 \cosh \frac{m\pi\lambda_1 R}{2} \cos \frac{m\pi\lambda_2 R}{2} \right] \tag{31b}$$

where

$$\phi_m = \cosh m\pi\lambda_1 R + \cos m\pi\lambda_2 R, \tag{32}$$

$$\lambda_1 = \sqrt{\frac{1+\eta}{2}}, \quad \lambda_2 = \sqrt{\frac{1-\eta}{2}}, \quad -1 < \eta < 1. \tag{33}$$

It is worth mentioning that the corresponding solutions for the maximum stresses σ_x and σ_y given in Lekhnitskii (1968) are erroneous. For cases in which $\eta > 1$, the maximum stresses are

$$\frac{\sigma_x h^2}{qb^2} = \frac{3\nu_{12}}{4} + \frac{24}{\pi^3 \lambda(\lambda_1^2 - \lambda_2^2)} \sum_{m=1,3,\ldots}^{\infty} \frac{(-1)^{(m-1)/2}}{m^3} \left[\frac{\lambda_2^2(\nu_{21} - \lambda_1^2\sqrt{\lambda})}{\cosh \frac{m\pi\lambda_1 R}{2}} - \frac{\lambda_1^2(\nu_{21} - \lambda_2^2\sqrt{\lambda})}{\cosh \frac{m\pi\lambda_2 R}{2}} \right] \tag{34a}$$

$$\frac{\sigma_y h^2}{qb^2} = \frac{3}{4} + \frac{24}{\pi(\lambda_1^2 - \lambda_2^2)} \sum_{m=1,3,\ldots}^{\infty} \frac{(-1)^{(m-1)/2}}{m^3} \left[\frac{\lambda_2^2(1 - \nu_{12}\lambda_1^2\sqrt{\lambda})}{\cosh \frac{m\pi\lambda_1 R}{2}} - \frac{\lambda_1^2(1 - \nu_{12}\lambda_2^2\sqrt{\lambda})}{\cosh \frac{m\pi\lambda_2 R}{2}} \right] \tag{34b}$$

where

$$\lambda_1 = \sqrt{\eta + \sqrt{\eta^2 - 1}}, \quad \lambda_2 = \sqrt{\eta - \sqrt{\eta^2 - 1}}, \quad 1 < \eta < \infty. \tag{35}$$

Note that $\lambda = 1$, $\eta = 1$ corresponds to the isotropic case; the corresponding solutions for σ_x and σ_y can be found in Timoshenko and Woinowsky-Krieger (1961). Note also that, no matter what value of η has, as the adjusted plate aspect ratio R becomes large ($R \geqslant 4$, say), we have $\sigma_x \to 3\nu_{12}qb^2/4h^2$, $\sigma_y \to 3qb^2/4h^2$.

Shown in Fig. 6a is the normalized maximum stress σ_x as a function of the plate aspect ratio a/b for $\lambda = 1$, $\eta = 0.414$, $h/b = 0.021$. The analytic solution (31a) is shown as the solid line, the isotropic solution ($\lambda = 1, \eta = 1$) as the dashed line, and the finite element results are shown as points. The finite element solution agrees well with the analytic solution given by (31a). Here again, even if $E_1 = E_2$, i.e., $\lambda = 1$, the isotropic solution can give rise to significant errors when the plate aspect ratio is close to unity. Similar plots are displayed in Fig. 6b for σ_y as a function of the plate aspect ratio; the features are the same as that exhibited in Fig. 6a.

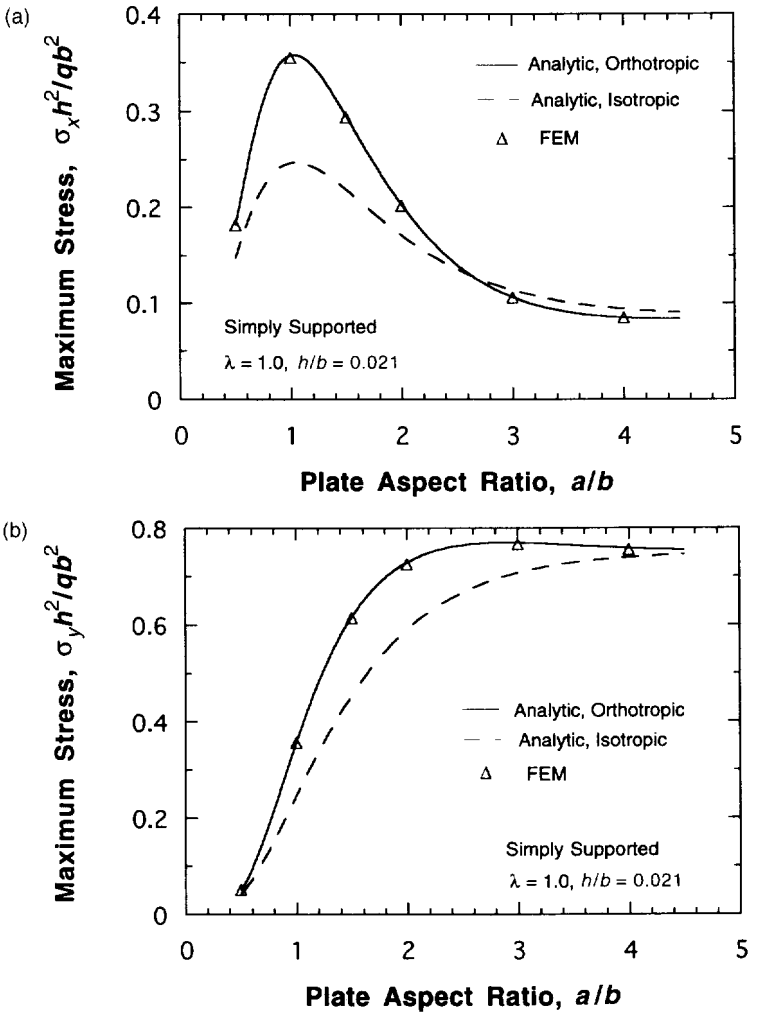

Fig. 6. Normalized maximum stresses σ_x in (a) and σ_y in (b), respectively, as a function of the plate aspect ratio a/b for $\lambda = 1$, $\eta = 0.414$, $h/b = 0.021$ for plates with all edges simply supported. The analytic orthotropic solution is shown as the solid line, the isotropic solution ($\lambda = 1, \eta = 1$) as the dashed line, and the finite element results are shown as points.

In general, the solutions for maximum stresses given in eqns (31) and (34) are accurate only for thin plates. However, it is found that for $h/b \leqslant 1/12$, the normalized maximum stress $\sigma_x h^2/qb^2$ and $\sigma_y h^2/qb^2$ are essentially independent of plate thickness h, as can be seen from Figs 7a and 7b.

4.2. *Plates with two edges clamped/others simply supported*

Considered in this subsection is a plate clamped along edges parallel to the y-axis and simply supported along the other two edges. Solutions for $w(x, y)$ can be found in Lekhnitskii (1968). Discussed below are the maximum deflection and the stresses at the center of the plate.

4.2.1. *Maximum deflection.* The maximum deflection of a plate with $-1 < \eta < 1$ has the form

$$\frac{\Delta}{\Delta_0} = \frac{5}{384} - \frac{8}{\pi^5} \sum_{m=1,3,\ldots}^{\infty} \frac{(-1)^{(m-1)/2}}{m^5 \psi_m} \left[\lambda_1 \cosh \frac{m\pi\lambda_1 R}{2} \sin \frac{m\pi\lambda_2 R}{2} + \lambda_2 \sinh \frac{m\pi\lambda_1 R}{2} \cos \frac{m\pi\lambda_2 R}{2} \right] \tag{36}$$

where

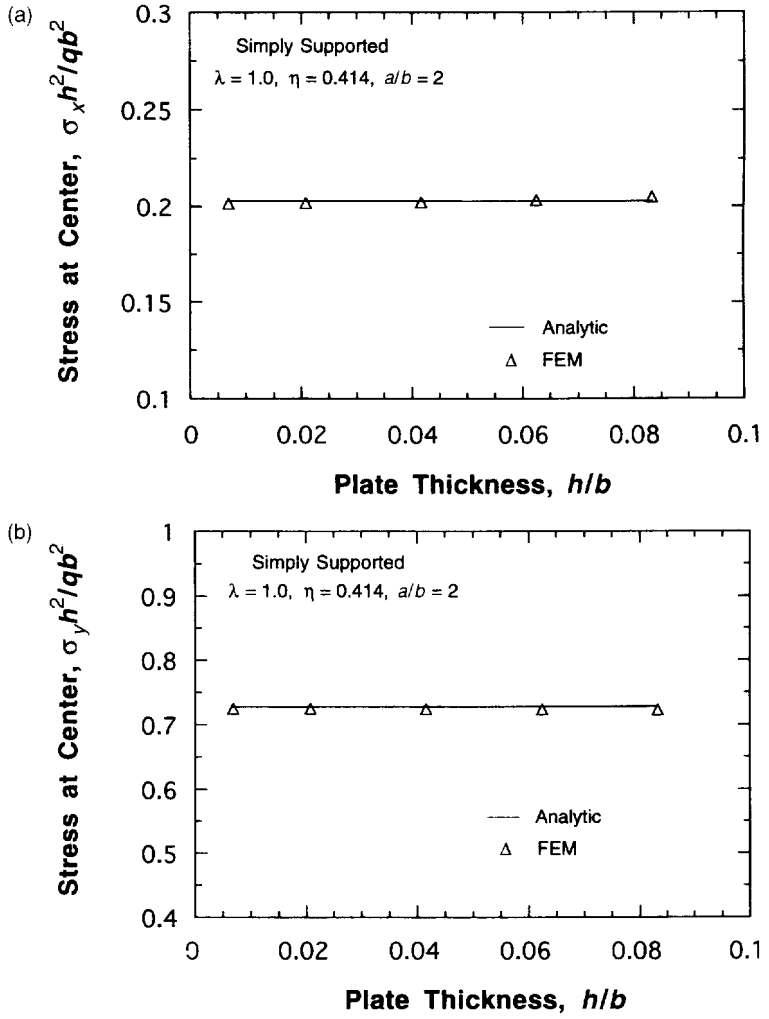

Fig. 7. Normalized maximum stresses σ_x in (a) and σ_y in (b), respectively, as a function of the nondimensional plate thickness h/b for $\lambda = 1$, $\eta = 0.414$, $a/b = 2$ for plates with all edges simply supported. The analytic solution is shown as the solid line, the finite element results are shown as points.

$$\psi_m = \lambda_2 \sinh m\pi\lambda_1 R + \lambda_1 \sin m\pi\lambda_2 R \tag{37}$$

with λ_1 and λ_2 given in (33). For a plate with $1 < \eta < \infty$, Δ/Δ_0 is given by

$$\frac{\Delta}{\Delta_0} = \frac{5}{384} - \frac{4}{\pi^5} \sum_{m=1,3,\ldots} \frac{(-1)^{(m-1)/2}}{m^5 \zeta_m} \left[\lambda_1 \sinh \frac{m\pi\lambda_1 R}{2} - \lambda_2 \sinh \frac{m\pi\lambda_2 R}{2} \right] \tag{38}$$

where

$$\zeta_m = \lambda_1 \sinh \frac{m\pi\lambda_1 R}{2} \cosh \frac{m\pi\lambda_2 R}{2} - \lambda_2 \cosh \frac{m\pi\lambda_1 R}{2} \sinh \frac{m\pi\lambda_2 R}{2} \tag{39}$$

and λ_1 and λ_2 are defined in (35). It is evident from eqns (36) and (38) that independent of η, Δ/Δ_0 tends to 5/384 when R becomes large (say, $R > 3$).

For comparison, the maximum deflection Δ/Δ_0 is plotted in Fig. 8a against the adjusted plate aspect ratio R for $\lambda = 1$, $\eta = 0.414$, $h/b = 0.021$. The finite element solution shown as points agrees well with the analytic solution shown as the solid line. The isotropic solution ($\lambda = 1, \eta = 1$), however, can have large errors even for a plate with $E_1 = E_2$. The normalized maximum deflection Δ/Δ_0 is found to be quite insensitive to the increase in plate thickness for $h/b \leqslant 1/12$. At $h/b = 1/12$, the relative error is just 5%, as can be seen from Fig. 8b.

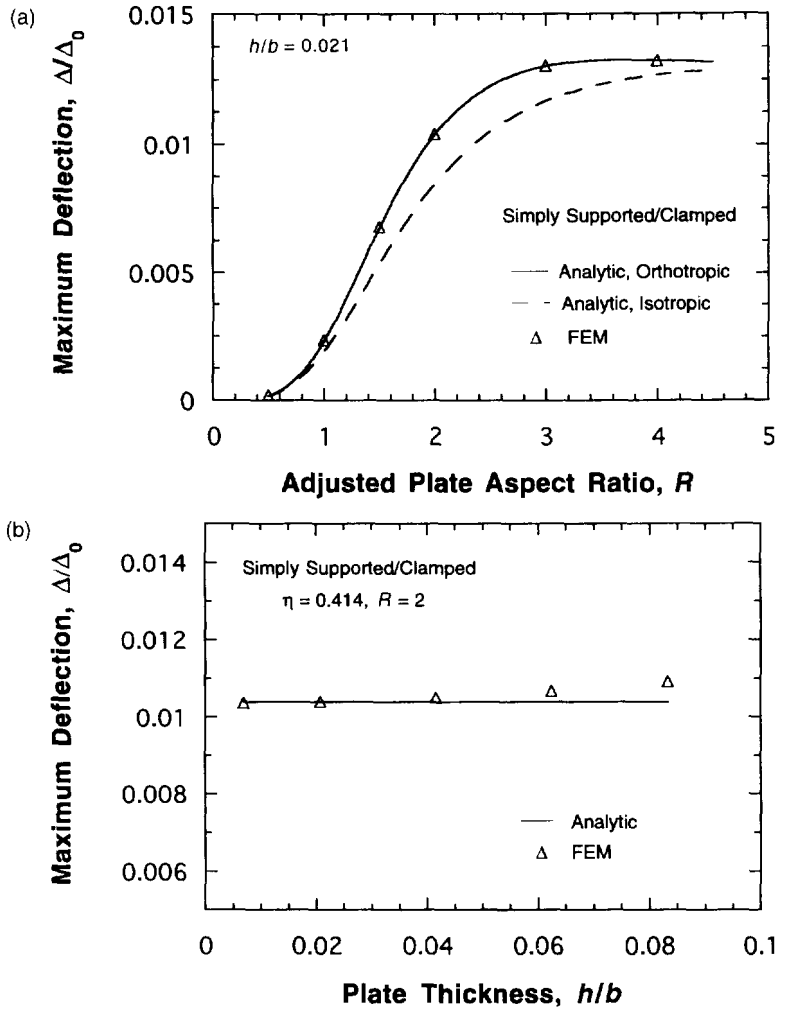

Fig. 8. Normalized maximum deflection Δ/Δ_0 as a function of (a) the adjusted plate aspect ratio $R = (D_{22}/D_{11})^{1/4} a/b$ and (b) the nondimensional plate thickness h/b for plates with two edges clamped and others simply supported. The analytic solution is shown as the solid line and the finite element solution as points. Shown also in (a) as the dashed line is the corresponding isotropic solution.

4.2.2. *Stresses at the center of the plate.* For a plate with two edges clamped and two other edges simply supported, if the material is isotropic, the maximum stresses (tensile or compressive) occur at the middle of the clamped edges. If the plate is orthotropic, however, the location at which the maximum stress occurs depends on plate aspect ratio and material orthotropy. In the following, only stresses at the center of the plate are considered; they may or may not be the maximum stresses.

When $-1 < \eta < 1$, the stresses at the center of the plate can be calculated from (Lekhnitskii, 1968)

$$\frac{\sigma_x h^2}{qb^2} = \frac{3\nu_{12}}{4} - \frac{48}{\pi^3 \lambda} \sum_{m=1,3,\ldots}^{\infty} \frac{(-1)^{(m-1)/2}}{m^3 \psi_m} \times \left[(\nu_{21} - \sqrt{\lambda})\lambda_1 \cosh\frac{m\pi\lambda_1 R}{2} \sin\frac{m\pi\lambda_2 R}{2} + (\nu_{21} + \sqrt{\lambda})\lambda_2 \sinh\frac{m\pi\lambda_1 R}{2} \cos\frac{m\pi\lambda_2 R}{2} \right] \quad (40a)$$

$$\frac{\sigma_x h^2}{qb^2} = \frac{3}{4} - \frac{48}{\pi^3} \sum_{m=1,3,\ldots}^{\infty} \frac{(-1)^{(m-1)/2}}{m^3 \psi_m} \times \left[(1 - \nu_{12}\sqrt{\lambda})\lambda_1 \cosh\frac{m\pi\lambda_1 R}{2} \sin\frac{m\pi\lambda_2 R}{2} + (1 + \nu_{12}\sqrt{\lambda})\lambda_2 \sinh\frac{m\pi\lambda_1 R}{2} \cos\frac{m\pi\lambda_2 R}{2} \right] \quad (40b)$$

where ψ_m is given in (37) and λ_1 and λ_2 are defined in (33).

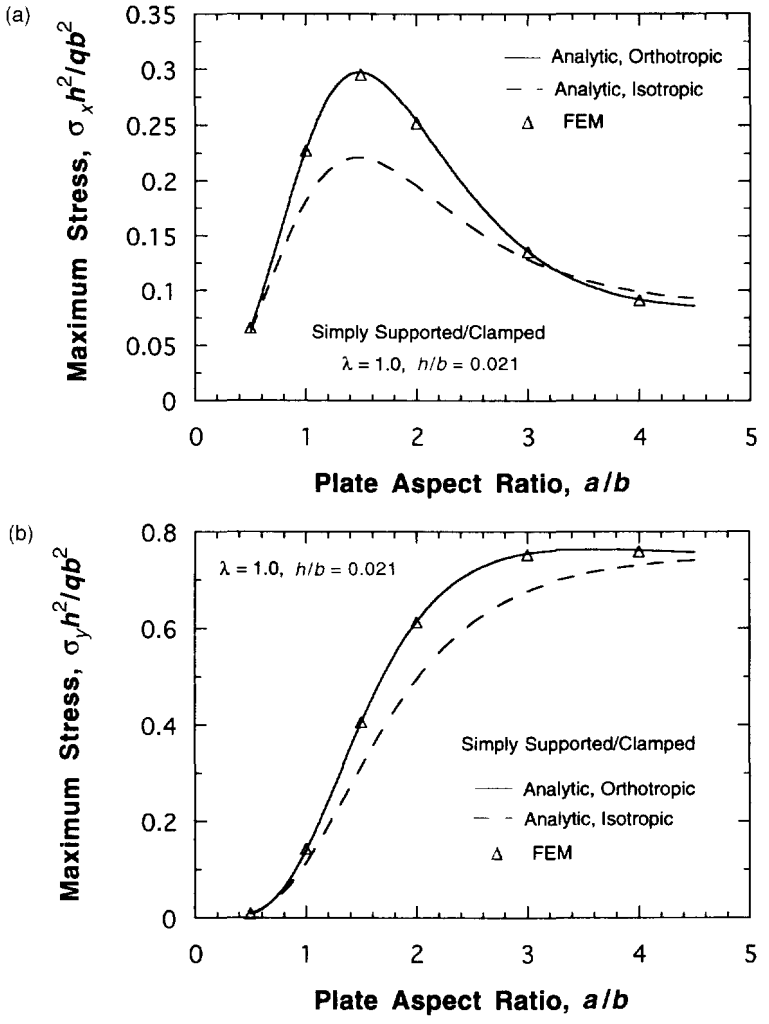

Fig. 9. Normalized maximum stresses σ_x in (a) and σ_y in (b), respectively, as a function of the plate aspect ratio a/b for $\lambda = 1$, $\eta = 0.414$, $h/b = 0.021$ for plates with two edges clamped and others simply supported. The analytic orthotropic solution is shown as the solid line, the isotropic solution ($\lambda = 1, \eta = 1$) as the dashed line, and the finite element results are shown as points.

For cases in which $\eta > 1$, the expressions for stresses at the center of the plate are given by (Lekhnitskii, 1968)

$$\frac{\sigma_x h^2}{qb^2} = \frac{3\nu_{12}}{4} + \frac{24}{\pi^3 \bar{\lambda}} \sum_{m=1,3,\ldots}^{\infty} \frac{(-1)^{(m-1)/2}}{m^3 \zeta_m} \left[(\nu_{21} - \lambda_1^2 \sqrt{\bar{\lambda}}) \lambda_2 \sinh \frac{m\pi\lambda_2 R}{2} - (\nu_{21} - \lambda_2^2 \sqrt{\bar{\lambda}}) \lambda_1 \sinh \frac{m\pi\lambda_1 R}{2} \right] \quad (41a)$$

$$\frac{\sigma_y h^2}{qb^2} = \frac{3}{4} + \frac{24}{\pi^3} \sum_{m=1,3,\ldots}^{\infty} \frac{(-1)^{(m-1)/2}}{m^3 \zeta_m} \left[(1 - \nu_{12} \lambda_1^2 \sqrt{\bar{\lambda}}) \lambda_2 \sinh \frac{m\pi\lambda_2 R}{2} - (1 - \nu_{12} \lambda_2^2 \sqrt{\bar{\lambda}}) \lambda_1 \sinh \frac{m\pi\lambda_1 R}{2} \right] \quad (41b)$$

where ζ_m is the same as that in (39) and λ_1 and λ_2 are given in (35). Here again, no matter what η is, when the adjusted plate aspect ratio R is such that $R \geqslant 4$, the stresses tend to $\sigma_x = 3\nu_{12} qb^2/4h^2$, $\sigma_y = 3qb^2/4h^2$.

A comparison is made in Fig. 9a for the normalized stress $\sigma_x h^2/qb^2$ obtained using eqn

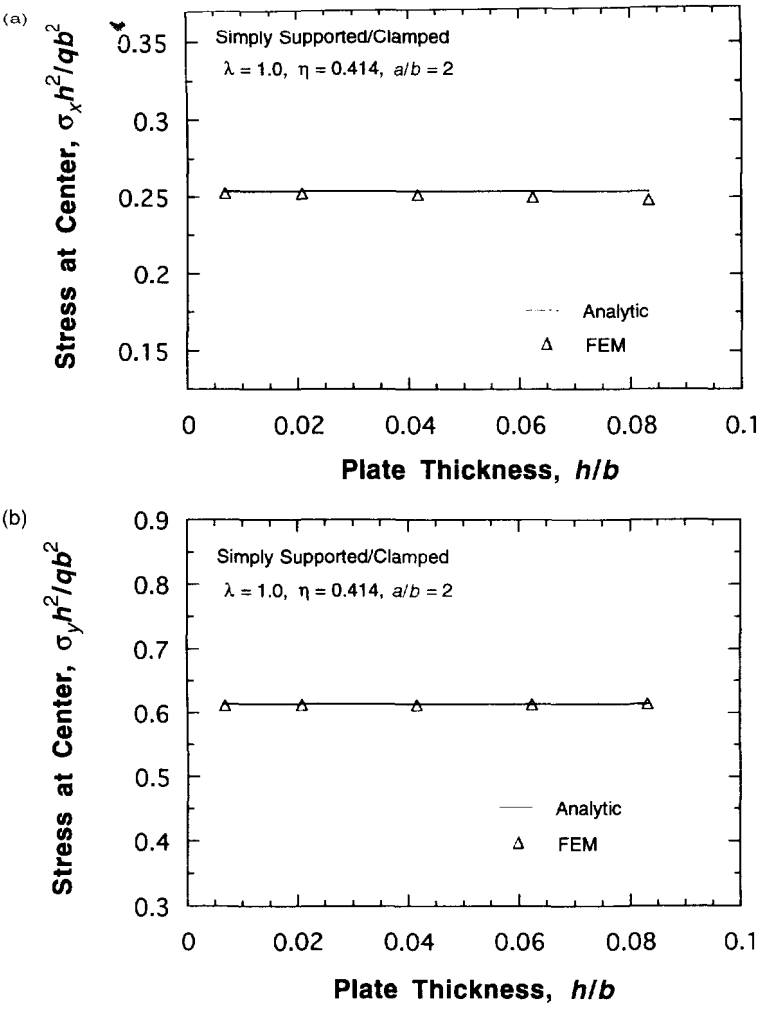

Fig. 10. Normalized maximum stresses σ_x in (a) and σ_y in (b), respectively, as a function of the nondimensional plate thickness h/b for $\lambda = 1$, $\eta = 0.414$, $a/b = 2$ for plates with two edges clamped and others simply supported. The analytic solution is shown as the solid line, the finite element results are shown as points.

(40a) (shown as the solid line) and using finite elements (shown as points). The corresponding solution based on the isotropic assumption is also displayed. The finite element solution is found to be almost identical to the analytic solution given in (40a); the isotropic approximation can lead to large errors even if $E_1 = E_2$ (i.e., $\lambda = 1$). The same features are true for the normalized stress $\sigma_y h^2/qb^2$ as can be seen from Fig. 9b. For $h/b \leqslant 1/12$, it is found that the normalized maximum stresses $\sigma_x h^2/qb^2$ and $\sigma_y h^2/qb^2$ are essentially independent of h, as demonstrated by Figs 10a and 10b.

4.3. *Plates with all edges clamped*

For a plate with all edges clamped, there exists no exact solution for the deflection $w(x, y)$. Approximate solutions have been developed based on various methods (Lekhnitskii, 1968; Whitney, 1987). Given below are solutions obtained using the Ritz method.

4.3.1. *Maximum deflection.* For a plate with $-1 < \eta < \sqrt{3.5}$, an approximate solution for the maximum deflection is derived (Appendix B)

$$\frac{\Delta}{\Delta_0} = \frac{1}{384}\left[1 - \frac{2\lambda_1 \cosh\frac{\lambda_1 R}{2}\sin\frac{\lambda_2 R}{2} + 2\lambda_2 \sinh\frac{\lambda_1 R}{2}\cos\frac{\lambda_2 R}{2}}{\lambda_1 \sin\lambda_2 R + \lambda_2 \sinh\lambda_1 R}\right] \tag{42}$$

where

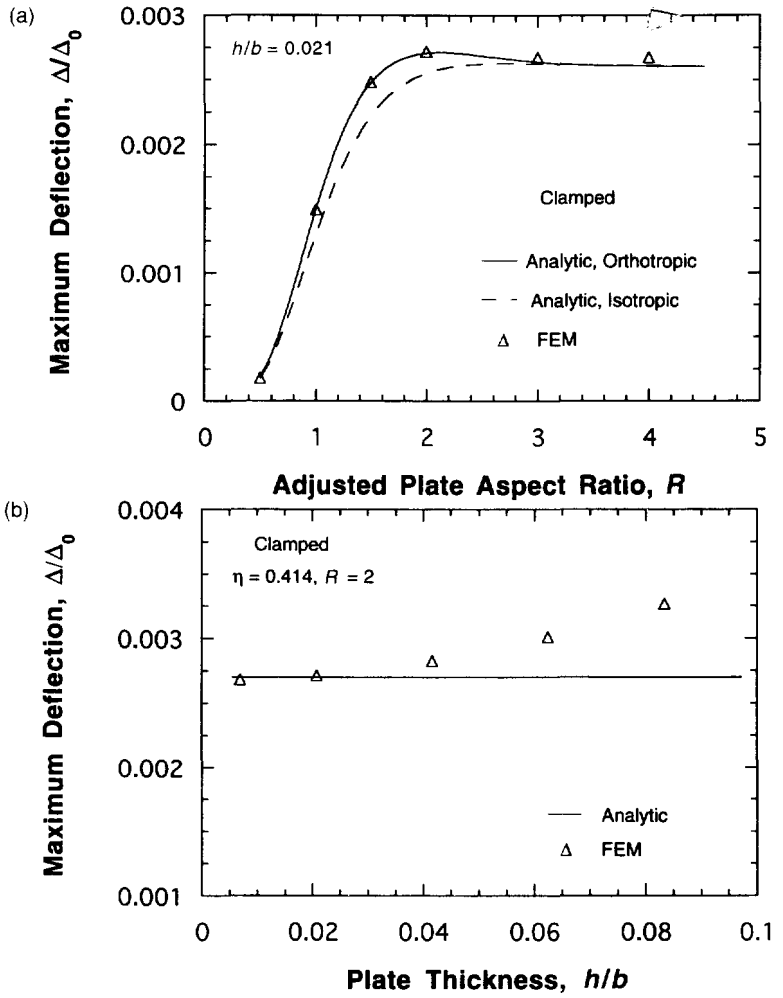

Fig. 11. Normalized maximum deflection Δ/Δ_0 as a function of (a) the adjusted plate aspect ratio $R = (D_{22}/D_{11})^{1/4} a/b$ and (b) the nondimensional plate thickness h/b for plates with all edges clamped. The analytic solution is shown as the solid line and the finite element solution as points. Shown also in (a) as the dashed line is the corresponding isotropic solution.

$$\lambda_1 = \sqrt{6(\sqrt{3.5}+\eta)}, \quad \lambda_2 = \sqrt{6(\sqrt{3.5}-\eta)}. \tag{43}$$

For a plate with $\eta > \sqrt{3.5}$, we have (Lekhnitskii, 1968)

$$\frac{\Delta}{\Delta_0} = \frac{1}{384}\left[1 - \frac{\lambda_1 \sinh\frac{\lambda_1 R}{2} - \lambda_2 \sinh\frac{\lambda_2 R}{2}}{\lambda_1 \sinh\frac{\lambda_1 R}{2}\cosh\frac{\lambda_2 R}{2} - \lambda_2 \sinh\frac{\lambda_2 R}{2}\cosh\frac{\lambda_1 R}{2}}\right] \tag{44}$$

where

$$\lambda_1 = 2\sqrt{3(\eta+\sqrt{\eta^2-3.5})}, \quad \lambda_2 = 2\sqrt{3(\eta-\sqrt{\eta^2-3.5})}. \tag{45}$$

Regardless of the value of η, as the adjusted plate aspect ratio R becomes large, say, $R > 3$, Δ/Δ_0 tends to 1/384.

To check the accuracy of the approximate solution (42), in Fig. 11a, the maximum deflections Δ/Δ_0 obtained using eqn (42) and the finite elements are plotted against the adjusted plate aspect ratio R for $\lambda = 1$, $\eta = 0.414$, $h/b = 0.021$. The finite element solution shown as points is believed to be very accurate as demonstrated by Figs (5a) and (8a); the results shown in Fig. 11a are obtained by merely changing the boundary conditions in the

model. Compared with the finite element results, the analytic solution is seen to be quite accurate for a wide range of plate aspect ratios. It is also evident that the effect of material orthotropy on the maximum deflection Δ is relatively weak, since the isotropic solution shown as the dashed line is quite close to the orthotropic solution. When the plate thickness increases, the error in Δ given by (42) increases owing to the thin plate theory assumptions, as demonstrated by Fig. 11b. At $h/b = 1/16$, the relative error is about 10%.

4.3.2. *Stresses at the center of the plate.* The stresses at the center of a plate with $-1 < \eta < \sqrt{3.5}$ can be calculated from the approximate solution for $w(x, y)$ (Appendix B)

$$\frac{\sigma_x h^2}{qb^2} = \frac{\nu_{12}}{4} - \frac{1}{8\lambda\omega}\left[(3\sqrt{3.5\lambda}+4\nu_{21})\lambda_2 \sinh\frac{\lambda_1 R}{2}\cos\frac{\lambda_2 R}{2} - (3\sqrt{3.5\lambda}-4\nu_{21})\lambda_1 \cosh\frac{\lambda_1 R}{2}\sin\frac{\lambda_2 R}{2}\right] \tag{46a}$$

$$\frac{\sigma_y h^2}{qb^2} = \frac{1}{4} - \frac{1}{8\omega}\left[(3\nu_{12}\sqrt{3.5\lambda}+4)\lambda_2 \sinh\frac{\lambda_1 R}{2}\cos\frac{\lambda_2 R}{2} - (3\nu_{12}\sqrt{3.5\lambda}-4)\lambda_1 \cosh\frac{\lambda_1 R}{2}\sin\frac{\lambda_2 R}{2}\right] \tag{46b}$$

where

$$\omega = \lambda_1 \sin\lambda_2 R + \lambda_2 \sinh\lambda_1 R \tag{47}$$

and λ_1 and λ_2 are given in (43). For plates with $\eta > \sqrt{3.5}$, the stresses at center of the plate are given by

$$\frac{\sigma_x h^2}{qb^2} = \frac{\nu_{12}}{4} - \frac{(16\nu_{21}-\lambda_2^2\sqrt{\lambda})\lambda_1 \sinh\frac{\lambda_1 R}{2} - (16\nu_{21}-\lambda_1^2\sqrt{\lambda})\lambda_2 \sinh\frac{\lambda_2 R}{2}}{64\lambda\left(\lambda_1 \sinh\frac{\lambda_1 R}{2}\cosh\frac{\lambda_2 R}{2} - \lambda_2 \sinh\frac{\lambda_2 R}{2}\cosh\frac{\lambda_1 R}{2}\right)} \tag{48a}$$

$$\frac{\sigma_y h^2}{qb^2} = \frac{1}{4} - \frac{(16-\nu_{12}\lambda_2^2\sqrt{\lambda})\lambda_1 \sinh\frac{\lambda_1 R}{2} - (16-\nu_{12}\lambda_1^2\sqrt{\lambda})\lambda_2 \sinh\frac{\lambda_2 R}{2}}{64\left(\lambda_1 \sinh\frac{\lambda_1 R}{2}\cosh\frac{\lambda_2 R}{2} - \lambda_2 \sinh\frac{\lambda_2 R}{2}\cosh\frac{\lambda_1 R}{2}\right)} \tag{48b}$$

where λ_1 and λ_2 are defined in (45). When the adjusted plate aspect ratio R is large, say, $R > 3$, we have $\sigma_x \approx \nu_{12} qb^2/4h^2$, $\sigma_y \approx qb^2/4h^2$.

Displayed in Fig. 12a is the normalized stress $\sigma_x h^2/qb^2$ as a function of the plate aspect ratio a/b for $h/b = 0.021$, $\lambda = 1$, $\eta = 0.414$. The analytic solution (46a) is shown as the solid line, the finite element solution the points, the solution based on the isotropic assumption is also shown as the dashed line for comparison. The isotropic solution, generated using the FORTRAN code developed by Steele (1994), is that given by Danielson *et al.* (1994) based on a Fourier expansion scheme. Although still approximate, the solution given by (46a) is seen to be quite accurate, especially when $a/b > 1$. The isotropic solution, however, can give rise to large errors when $a/b \approx 1.0$. A similar comparison is made in Fig. 12b for $\sigma_y h^2/qb^2$ as a function of a/b. The analytic solution given by (46b) agrees well with the finite element results. Evidently, the isotropic solutions for σ_x and σ_y provide a good approximation only for $a/b > 2.5$. Shown in Figs 13a, b are the effects of plate thickness h on the normalized stresses $\sigma_x h^2/qb^2$ and $\sigma_y h^2/qb^2$, respectively. Clearly, for $h \leqslant b/12$, $\sigma_y h^2/qb^2$ is essentially independent of h.

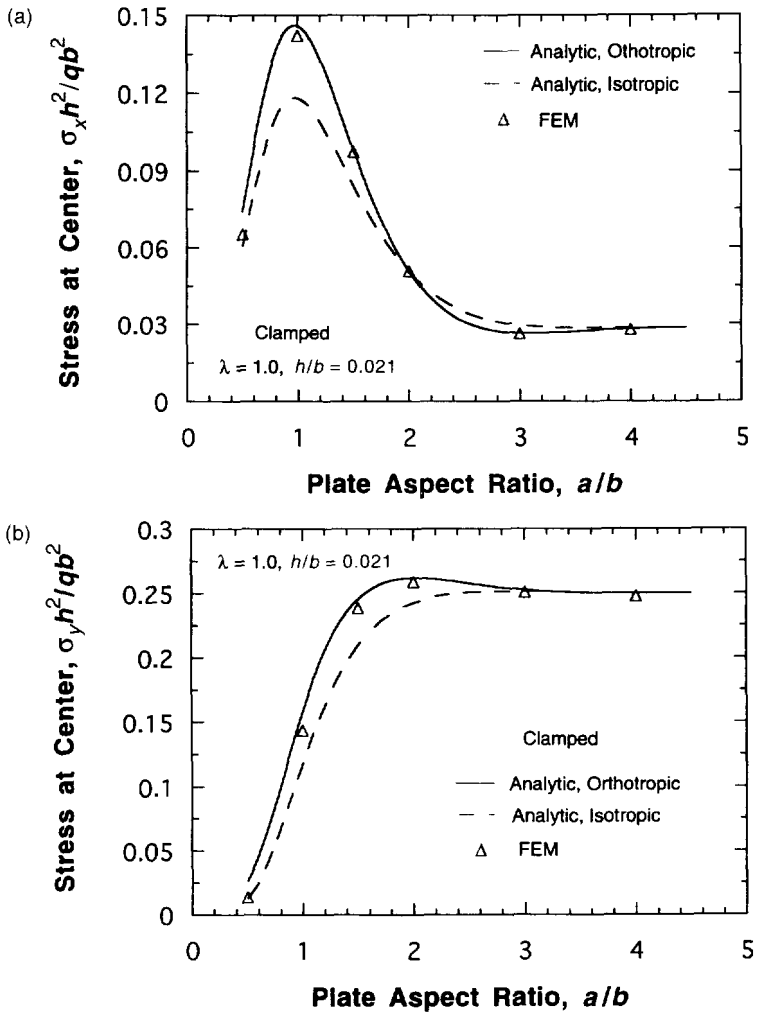

Fig. 12. Normalized maximum stresses σ_x in (a) and σ_y in (b), respectively, as a function of the plate aspect ratio a/b for $\lambda = 1$, $\eta = 0.414$, $h/b = 0.021$ for plates with all edges clamped. The analytic orthotropic solution is shown as the solid line, the isotropic solution ($\lambda = 1, \eta = 1$) as the dashed line, and the finite element results are shown as points.

To further demonstrate the accuracy of the approximate solution developed in Appendix B for bending of an all-edges-clamped orthotropic plate with $-1 < \eta < \sqrt{3.5}$, distributions of the stresses σ_x and σ_y along the x-direction at the surface of the plate in the symmetry plane $y = b/2$ are calculated for an isotropic plate (i.e., $\lambda = 1, \eta = 1$) with $a/b = 2$, Poisson's ratio $\nu = 0.115$ using eqns (B17) and (B18). These distributions are also obtained using the FORTRAN code developed by Steele (1994) based on a Fourier expansion scheme (Danielson *et al.*, 1994). Shown in Fig. 14a is the comparison of the approximate and the Fourier series solutions for σ_x as a function of position x in the plate at $y = b/2$ (the symmetry plane). It is seen that the two solutions are in good agreement; they are essentially identical for $-0.3a < x < 0.3a$ where a is the length of the plate. A similar comparison for σ_y is given in Fig. 14b, and the overall agreement between the two solutions is also quite good.

5. CONCLUDING REMARKS

Composite plates made of solid laminates, sandwich laminates, and laminates reinforced with stiffeners are widely used in aerospace and marine structures. To guide the design of these composite structures, in this article, existing analytical solutions for bending

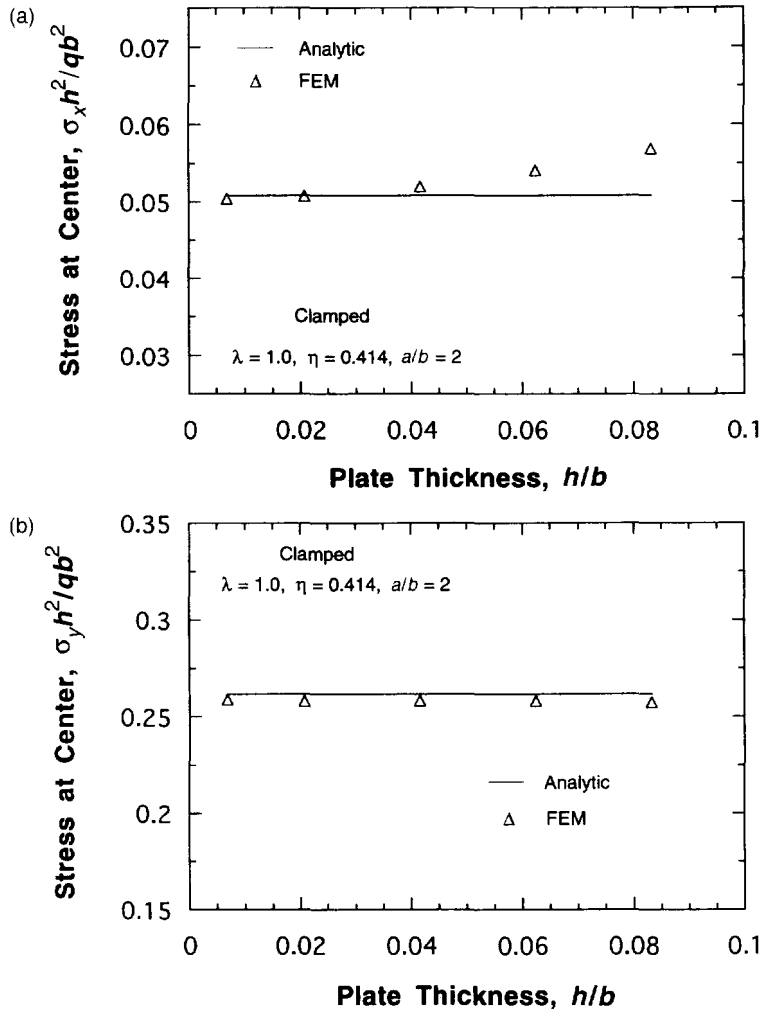

Fig. 13. Normalized maximum stresses σ_x in (a) and σ_y in (b), respectively, as a function of the nondimensional plate thickness h/b for $\lambda = 1$, $\eta = 0.414$, $a/b = 2$ for plates with all edges clamped. The analytic solution is shown as the solid line, the finite element results are shown as points.

and buckling of unstiffened rectangular orthotropic thin plates are compiled and new solutions developed based on two non-dimensional orthotropic parameters λ and η. Systematic comparisons are made between analytic and finite element solutions for the critical buckling load under in-plane uniaxial compression, and deflection and stresses under out-of-plane uniform pressure. The accuracy of the analytic and finite element solutions is checked; the dependence of these solutions on plate aspect ratio and thickness is examined.

The solutions for critical buckling load, deflection and stresses of a composite plate depend on material orthotropy. To simplify the analysis, in this study, the material orthotropy of the plate is characterized by two non-dimensional parameters, λ and η. By using an orthotropy rescaling technique, only η appears in the governing equation. In addition, if $\eta \approx 1$, solutions for an orthotropic plate can be obtained directly from the corresponding isotropic results. When $\eta \neq 1$, the dependence on η can be quantified using analytical solutions or by performing a finite element analysis. For buckling of a plate under uniaxial compression, it is found that the effect of $\lambda = D_{22}/D_{11}$ is just to modify the plate aspect ratio in terms of $R = \lambda^{1/4} a/b$; decreasing λ will reduce the number of half-waves and in general increase σ_{cr}. The effect of η is to move the σ_{cr} vs R curve up or down: a larger η results in a higher σ_{cr}.

Some of the analytic solutions discussed in this article are exact solutions for thin plates; others are approximate solutions with different degrees of accuracy. Specifically,

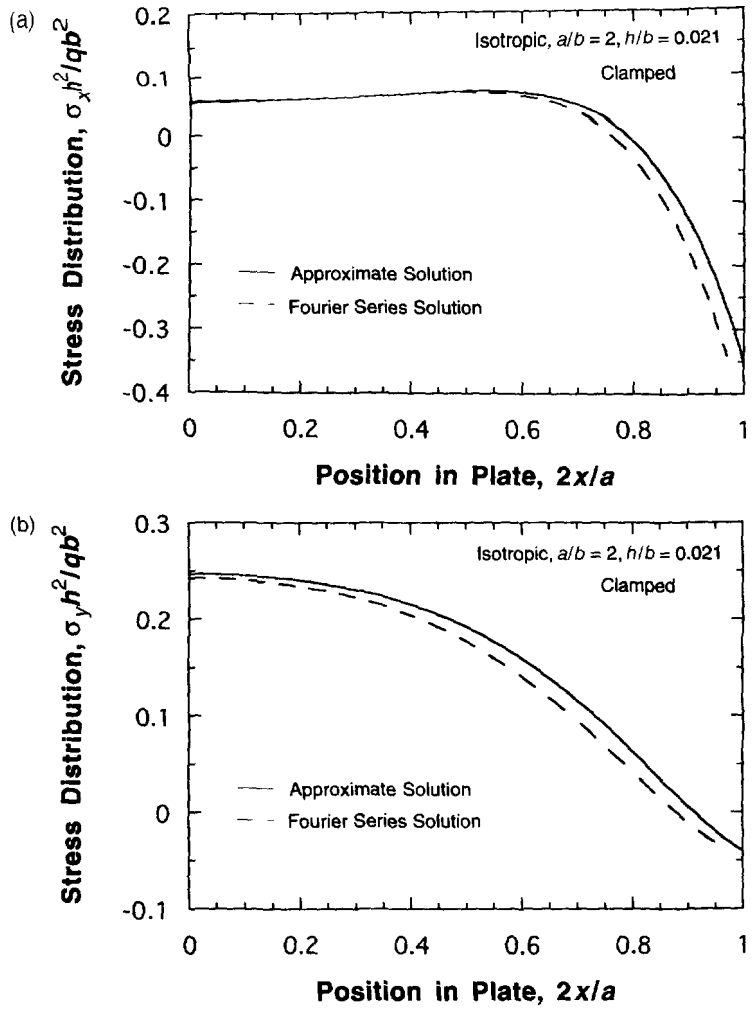

Fig. 14. Normalized stress distributions $\sigma_x(x)$ in (a) and $\sigma_y(x)$ in (b), respectively, as a function of the position x at the symmetry plane of the plate for a clamped isotropic plate with $a/b = 2$, $h/b = 0.021$. The approximate analytic solution is shown as the solid line, the Fourier series solution as the dashed line.

for plates with all edges simply supported, and for plates with two edges simply supported and others clamped, the analytic solutions compiled for critical buckling load, the maximum deflection and the stresses at the center of the plate are exact, although many of them are series solutions. For plates with all edges clamped, the analytic solutions are approximate. The accuracy of the analytic solutions for the maximum deflection and stresses is found to be quite good. However, the analytic solution for the critical buckling load is neither accurate nor conservative. A better solution for buckling of thin plates with all edges clamped needs to be developed.

There are three purposes of carrying out finite element analyses in this study for bending and buckling of orthotropic thin plates. First, with available exact analytic solutions for simply supported thin plates, the accuracy of the finite element model is established. The same finite element model is then used to obtain solution for plates with all edges clamped by changing the boundary conditions. Second, the accuracy of the approximate analytic solutions are checked by comparing them with the more precise finite element results. Third, for plates with relatively large thicknesses, the finite element results are more accurate, since the finite element S4R used in the calculations is valid for both thin and thick plates. It is well recognized that the finite element solutions are not exact in the strict mathematical sense. However, the results obtained using finite elements are believed to be very accurate and thus can be used to check the accuracy of the approximate analytic solutions.

All the analytic solutions presented in this paper are based on the thin plate theory assumptions; they are valid only for certain range of plate thicknesses. For critical buckling stress σ_{cr} and the maximum deflection Δ of a plate, such a range depends on boundary conditions of the plate. For a plate with all edges simply supported, the analytic solutions for σ_{cr} and Δ are accurate even when the plate thickness is relatively large (say, $h = b/12$). If a plate has two simply supported and two clamped edges, the thickness dependence is stronger, i.e., the analytic solutions for σ_{cr} and Δ are good for a smaller range of plate thicknesses. For a plate with all edges clamped, the analytic solutions for σ_{cr} and Δ defer from finite element results even for a relatively thin plate. It is also revealed that for all the boundary conditions considered (all edges simply supported, all edges clamped, and simply supported/clamped), the stresses in the middle of the plate are essentially independent of the plate thickness if $h \leqslant b/12$. For thick plates, analytic solutions have been developed using a shear deformation plate theory (Reddy, 1984; Whitney, 1987); the discussion of such solutions, however, is out of the scope of the present study.

Acknowledgements –This work was supported in part by the Naval Surface Warfare Center (NSWC), Carderock under contract No. N00039-94-C-001 in support of the Organic Composites Ship Structures Project, and in part by NSF through a Research Initiation Award MSS 9210250 to G. Bao. Special thanks go to Professor C. R. Steele for allowing us to use the FORTRAN code he developed for clamped plates. Helpful discussions with C. R. Steele and D. A. Danielson are gratefully acknowledged.

REFERENCES

Bao, G., Ho, S., Suo, Z. and Fan, B. (1992). The role of material orthotropy in fracture specimens for composites. *International Journal of Solids and Structures* **29**, 1105–1116.

Brunelle, E. J. and Oyibo, G. A. (1983). Generic buckling curves for specially orthotropic rectangular plates. *AIAA Journal* **21**, 1150–1156.

Danielson, D. A., Steele, C. R., Fakhroo, F. and Cricelli, A. S. (1994). Stresses in ship plating. *Technical Report NPS-MA-94-008*, Naval Postgraduate School, Monterey, CA.

Huber, M. T. (1929). *Probleme der Statik Technisch Wichtiger Orthotroper Platten*. Warszawa.

Jiang, W., Bao, G. and Roberts, J. (1996). Finite element modeling of stiffened and unstiffened orthotropic plates. *Computers and Structures*, in press.

Jones, R. M. (1975). *Mechanics of Composite Materials*, McGraw-Hill, New York.

Lekhnitskii, S. G. (1968). *Anisotropic Plates*, Gordon and Breach, Science Publishers, New York.

Lekhnitskii, S. G. (1981). *Theory of Elasticity of an Anisotropic Body*, Mir Publishers, Moscow.

March, H. W. and Smith, C. B. (1945). Buckling loads of flat sandwich panels in compression. *Forest Products Laboratory Report No.* 1525, Madison, Wisconsin.

Reddy, J. N. (1984). A refined nonlinear theory of plates with transverse shear deformation. *International Journal of Solids and Structures* **20**, 881–896.

Smith, C. S. (1990). *Design of Marine Structures in Composite Materials*, Elsevier Applied Science, London.

Steele, C. R. (1994). FORTRAN Program PLATE6 for computation of a clamped rectangular plate with pressure load and axial resultant force. Stanford University.

Suo, Z., Bao, G., Fan, B. and Wang, T. C. (1991). Orthotropy rescaling and implications for fracture in composites. *International Journal of Solids and Structures* **28**, 235–248.

Timoshenko, S. P. and Woinowsky-Krieger, S. (1959). *Theory of Plates and Shells*, McGraw-Hill, New York.

Timoshenko, S. P and Gere, J. M. (1961). *Theory of Elastic Stability*, McGraw-Hill, New York.

Whitney, J. M. (1987). *Structural Analysis of Laminated Anisotropic Plates*, Technomic Publishing, Lancaster.

Yu, S. D. and Cleghorn, W. L. (1993). Generic free vibration of orthotropic rectangular plates with clamped and simply supported edges. *Journal of Sound and Vibration* **163**, 439–450.

APPENDIX A

Consider a rectangular, orthotropic plate with length a and width b subjected to uniaxial compression $N_x (N_x > 0)$ in the x-direction, as shown in Fig. 1b. The loaded edges are clamped and other edges simply supported. After orthotropy rescaling, the governing equation for the deflection w is given by

$$\frac{\partial^4 w}{\partial x^4} + 2\eta \frac{\partial^4 w}{\partial x^2 \partial y^2} + \frac{\partial^4 w}{\partial y^4} + \frac{N_x}{D_{11}} \frac{\partial^2 w}{\partial x^2} = 0. \tag{A1}$$

Assuming that

$$w(x, y) = f(x) \sin \frac{\pi y}{\hat{b}}, \tag{A2}$$

where $\hat{b} = \lambda^{-1/4} b$, λ and η are the non-dimensional parameters defined in (9a); the boundary conditions at the two simply supported edges ($y = 0, \hat{b}$) are satisfied. Substituting (A2) into (A1), one obtains the equation for $f(x)$

$$\frac{d^4 f}{dx^4} + 2\left(\frac{N_x}{2D_{11}} - \eta\frac{\pi^2}{\hat{b}^2}\right)\frac{d^2 f}{dx^2} + \frac{\pi^4}{\hat{b}^4} f = 0. \tag{A3}$$

The solution for $f(x)$ has the form

$$f(x) = e^{sx\pi/\hat{b}} \tag{A4}$$

where the characteristic equation for s is

$$s^4 + 2ks^2 + 1 = 0 \tag{A5}$$

with k defined by

$$k = \frac{\hat{b}^2 N_x}{2\pi^2 D_{11}} - \eta. \tag{A6}$$

When buckling occurs,

$$N_x = N_{cr} = \sigma_{cr} h, \tag{A7}$$

we thus have from (A6)

$$\frac{\sigma_{cr}}{\sigma_0} = 2(k + \eta) \tag{A8}$$

where σ_0 is a reference buckling stress defined in (18). Assuming that $k > 1$, the solutions of (A5) for s are given by

$$s = \pm i\lambda_1, \quad s = \pm i\lambda_2 \tag{A9}$$

$$\lambda_1 = \sqrt{k + \sqrt{k^2 - 1}}, \quad \lambda_2 = \sqrt{k - \sqrt{k^2 - 1}}. \tag{A10}$$

$f(x)$ is thus given by

$$f(x) = A\sin\lambda_1\frac{\pi}{\hat{b}}x + B\cos\lambda_1\frac{\pi}{\hat{b}}x + C\sin\lambda_2\frac{\pi}{\hat{b}}x + D\cos\lambda_2\frac{\pi}{\hat{b}}x. \tag{A11}$$

Applying the boundary conditions

$$w|_{x=0,a} = 0, \quad \left.\frac{\partial w}{\partial x}\right|_{x=0,a} = 0 \tag{A12}$$

to (A2) and (A11) and requiring a non-trivial solution for $f(x)$ leads to the equation for k

$$(1+k)\cos[(\lambda_1 - \lambda_2)\pi R] + (1-k)\cos[(\lambda_1 + \lambda_2)\pi R] = 2 \tag{A13}$$

where $R = \lambda^{1/4} a/b$ is the adjusted plate aspect ratio.

APPENDIX B

For a plate with all edges clamped, there exists no exact solution for the deflection w of the plate under uniform out-of-plane pressure. An approximate solution obtained based on the Ritz method is given in Lekhnitskii (1968). That solution, however, is only applicable for plates with $\eta > \sqrt{3.5}$. For most engineering composites such as fiber reinforced plastics, $\eta < \sqrt{3.5}$. It is thus necessary to develop an analytic solution for the regime $-1 < \eta < \sqrt{3.5}$.

The governing equation for the deflection w of a plate of length a and width b under uniform out-of-plane pressure q is given by

$$\frac{\partial^4 w}{\partial x^4} + 2\eta\frac{\partial^4 w}{\partial x^2 \partial y^2} + \frac{\partial^4 w}{\partial y^4} = \frac{q}{D_{11}}, \quad -a/2 < x < a/2, 0 < y < \hat{b} \tag{B1}$$

where the y-axis has been rescaled: the plate now has width $\hat{b} = \lambda^{1/4} b$. The boundary conditions are

$$w|_{x=-a/2} = 0, \quad w|_{y=0,\hat{b}} = 0, \quad \left.\frac{\partial w}{\partial x}\right|_{x=-a/2} = 0, \quad \left.\frac{\partial w}{\partial y}\right|_{y=0,\hat{b}} = 0. \tag{B2}$$

Assuming that

$$w(x,y) = \frac{q}{24D_{11}}(y^4 - 2\hat{b}y^3 + \hat{b}^2y^2)\phi(x), \tag{B3}$$

then the boundary conditions at $y = 0, \hat{b}$ are satisfied. Define

$$\psi(y) = y^4 - 2\hat{b}y^3 + \hat{b}^2y^2 \tag{B4}$$

and require that

$$\int_0^{\hat{b}} \left[\frac{\partial^4 w}{\partial x^4} + 2\eta\frac{\partial^4 w}{\partial x^2\partial y^2} + \frac{\partial^4 w}{\partial y^4} - \frac{q}{D_{11}}\right]\psi(y)\,dy = 0 \tag{B5}$$

we have the differential equation for $\phi(x)$

$$\frac{\hat{b}^4}{504}\frac{d^4\phi}{dx^4} - \frac{\eta\hat{b}^2}{21}\frac{d^2\phi}{dx^2} + \phi = 1. \tag{B6}$$

Let

$$\phi(x) = 1 + \exp\left(s\frac{x}{\hat{b}}\right), \tag{B7}$$

the characteristic equation for s is given by

$$\frac{1}{504}s^4 - \frac{\eta}{21}s^2 + 1 = 0. \tag{B8}$$

For $-1 < \eta < \sqrt{3.5}$, the solutions for s are

$$s = \pm(\lambda_1 \pm i\lambda_2) \tag{B9}$$

where

$$\lambda_1 = \sqrt{6(\sqrt{3.5} + \eta)}, \quad \lambda_2 = \sqrt{6(\sqrt{3.5} - \eta)}. \tag{B10}$$

Symmetry conditions in the x-direction implies that $\phi(x)$ can be expressed as

$$\phi(x) = 1 + A\cosh\left(\lambda_1\frac{x}{\hat{b}}\right)\cos\left(\lambda_2\frac{x}{\hat{b}}\right) + B\sinh\left(\lambda_1\frac{x}{\hat{b}}\right)\sin\left(\lambda_2\frac{x}{\hat{b}}\right). \tag{B11}$$

Applying the boundary conditions at $x = \pm a/2$, one obtains

$$A = -2\frac{\lambda_1\cosh\left(\frac{\lambda_1 R}{2}\right)\sin\left(\frac{\lambda_2 R}{2}\right) + \lambda_2\sinh\left(\frac{\lambda_1 R}{2}\right)\cos\left(\frac{\lambda_2 R}{2}\right)}{\lambda_1\sin(\lambda_2 R) + \lambda_2\sinh(\lambda_1 R)}, \tag{B12}$$

$$B = 2\frac{\lambda_1\sinh\left(\frac{\lambda_1 R}{2}\right)\cos\left(\frac{\lambda_2 R}{2}\right) - \lambda_2\cosh\left(\frac{\lambda_1 R}{2}\right)\sin\left(\frac{\lambda_2 R}{2}\right)}{\lambda_1\sin(\lambda_2 R) + \lambda_2\sinh(\lambda_1 R)} \tag{B13}$$

where $R = \lambda^{1/4}a/b$. The maximum deflection occurs at $x = 0, y = \hat{b}/2$

$$\Delta = w_{max} = \frac{qb^4}{384D_{22}}[1 + A]. \tag{B14}$$

The stresses at the surfaces of the plate can be obtained readily from (B3), (B11) (B13) and (15)–(16).

$$\sigma_x = \frac{6M_x}{h^2}, \quad \sigma_y = \frac{6M_y}{h^2}. \tag{16}$$

$$M_x = -D_{11}\frac{\partial^2 w}{\partial x^2} - \frac{D_{12}}{\sqrt{\lambda}}\frac{\partial^2 w}{\partial y^2} \tag{15a}$$

$$M_y = -D_{12}\frac{\partial^2 w}{\partial x^2} - \frac{D_{22}}{\sqrt{\lambda}}\frac{\partial^2 w}{\partial y^2} \tag{15b}$$

where

$$\frac{\partial^2 w}{\partial y^2} = \frac{q}{12D_{11}}(6y^2 - 6y\hat{h} + \hat{h}^2) \times \left[1 + A\cosh\frac{\lambda_1 x}{\hat{h}}\cos\frac{\lambda_2 x}{\hat{h}} + B\sinh\frac{\lambda_1 x}{\hat{h}}\sin\frac{\lambda_2 x}{\hat{h}}\right] \tag{B15}$$

$$\frac{\partial^2 w}{\partial x^2} = \frac{q}{24D_{11}\hat{h}^2}(y - \hat{h})^2 y^2$$
$$\times \left[((\lambda_1^2 - \lambda_2^2)A + 2\lambda_1\lambda_2 B)\cosh\frac{\lambda_1 x}{\hat{h}}\cos\frac{\lambda_2 x}{\hat{h}} + ((\lambda_1^2 - \lambda_2^2)B - 2\lambda_1\lambda_2 A)\sinh\frac{\lambda_1 x}{\hat{h}}\sin\frac{\lambda_2 x}{\hat{h}}\right]. \tag{B16}$$

In particular, at the symmetry plane $y = \hat{h}/2$

$$\frac{\sigma_x \hat{h}^2}{q\hat{h}^2} = \frac{\nu_{12}}{4} - \frac{1}{64\lambda}[\sqrt{\lambda}A(\lambda_1^2 - \lambda_2^2) + 2\sqrt{\lambda}B\lambda_1\lambda_2 - 16\nu_{21}A]\cosh\frac{\lambda_1 x}{\hat{h}}\cos\frac{\lambda_2 x}{\hat{h}}$$
$$- \frac{1}{64\lambda}[\sqrt{\lambda}B(\lambda_1^2 - \lambda_2^2) - 2\sqrt{\lambda}A\lambda_1\lambda_2 - 16\nu_{21}B]\sinh\frac{\lambda_1 x}{\hat{h}}\sin\frac{\lambda_2 x}{\hat{h}} \tag{B17}$$

$$\frac{\sigma_x \hat{h}^2}{q\hat{h}^2} = \frac{1}{4} - \frac{1}{64}[\nu_{12}\sqrt{\lambda}A(\lambda_1^2 - \lambda_2^2) + 2\nu_{12}\sqrt{\lambda}B\lambda_1\lambda_2 - 16A]\cosh\frac{\lambda_1 x}{\hat{h}}\cos\frac{\lambda_2 x}{\hat{h}}$$
$$- \frac{1}{64}[\nu_{12}\sqrt{\lambda}B(\lambda_1^2 - \lambda_2^2) - 2\nu_{12}\sqrt{\lambda}A\lambda_1\lambda_2 - 16B]\sinh\frac{\lambda_1 x}{\hat{h}}\sin\frac{\lambda_2 x}{\hat{h}}. \tag{B18}$$